Revision 1

Apatite trace element and isotope applications to petrogenesis and provenance

Emilie Bruand[1,2], Mike Fowler[2], Craig Storey[2] and James Darling[2]

[1]Department of Earth Sciences, University of Oxford , South Parks Road, Oxford, OX1 3AN [2]School of Earth and Environmental Sciences, Portsmouth University, Burnaby Building, Burnaby Road, Portsmouth PO1 3QL (UK)

Abstract

Apatite is an excellent tracer of petrogenetic processes as it can incorporate a large range of elements that are sensitive to melt evolution (LREE-MREE, Sr, Pb, Mn, halogens, Nd isotopes). Recent advances in the understanding of trace element concentrations and isotope ratios in apatite provide a novel tool to investigate magmatic petrogenesis and sediment provenance. Recent experimental work has better characterized trace element partition coefficients for apatite which are sensitive to changes in magma composition (e.g. SiO_2 and the Aluminium Saturation Index value). The chemistry of apatites from granitoids has been suggested to reflect the composition of the host magma and yield information about petrogenetic processes that are invisible at the whole rock scale (mixing, in-situ crystal fractionation, metasomatism). Nd isotopes in apatite can now be analysed by LA-MC-ICP-MS to constrain mantle and crustal contributions to the source(s) of the studied magma. These recent advances highlight exciting new horizons to understand igneous processes using accessory minerals. In this contribution, we use

a compilation of recent data to show that apatite in the matrix and as inclusions within zircon and titanite is useful for providing insights into the nature and petrogenesis of the parental magma. Trace element modelling from in-situ analyses of apatite and titanite can reliably estimate the original magma composition, using appropriate partition coefficients and careful imaging. This provides a new way to look at magmatic petrogenesis that have been overprinted by metamorphic processes. It also provides the rationale for new investigations of sedimentary provenance using detrital accessory minerals, and could provide a powerful new window into early Earth processes if applied to Archean or Hadean samples.

Keywords: apatite, petrogenesis, inclusions in accessory minerals, crustal evolution, provenance.

Introduction

Interest in apatite has recently increased as this mineral seems to be an excellent recorder of Earth and planetary processes (e.g. Bruand et al., 2014; Harlov et al., 2015; Mc Cubbin et al., 2015; Piccoli et al., 2015; Tartèse et al., 2014; Zirner et al., 2015). Development of in situ techniques such as laser ablation (LA)-ICP-MS and the ion microprobe allows analysis of trace elements in different zones within accessory minerals such as apatite that may record different parts of the crystallization history. Apatite has been shown to record petrogenetic processes during crystallisation (in-situ crystal fractionation, mixing, metasomatism) and is a mineral able to highlight events that are not always visible using whole rock compositions (Bruand et al., 2014). Apatite is also a datable mineral (by U-Pb) and recent

advances in that field have also been successful (e.g. Chew and Donelick, 2012). Developing petrological tools based on apatite chemistry is of broad interest as it is a common mineral in most igneous rock types (e.g. felsic, mafic, ultramafic; see Piccoli and Candela, 2002 for review), constitutes one of the main carriers of P_2O_5 and REE (alongside zircon, titanite, allanite and monazite), contains various elements sensitive to oxidation state (Mn, V, S; E.g. Miles et al., 2014, Parat et al., 2011) and can accommodate halogens in its structure (F and Cl).

In this contribution we compile recent findings showing that apatite is a valuable mineral for tracking igneous petrogenesis and is also of great potential use for provenance studies (Foster and Carter, 2007; Morton and Yaxley, 2007). The first part of this paper is dedicated to the use of apatite as a petrogenetic tool within granitoids and its ability to record different processes that are not necessarily visible using whole rock compositions. The second part looks at using apatite inclusions armoured within robust minerals (e.g. zircon, titanite) to provide a new provenance tool via characterization of the original host rock.

Apatite: A petrogenetic recorder

Imaging

Apatite is commonly zoned as a result of its crystallization, dissolution and/or reprecipitation history. Such zoning can be easily identified by imaging using back-scattered (BSE) and/or cathodoluminescence (CL) techniques (Fig. 1) and interpretation of this zoning combined with detailed petrographic study of the surrounding mineral phases can give additional information on the timing and

92 nature of apatite crystallization (e.g. Bruand et al., 2014; Zirner et al., 2015). In
93 Figure 1a, imaging of apatite crystals within a granitoid from high Ba-Sr granites
94 (northern Scotland) reveals distinct core and rim zonation, the significance of which
95 is discussed below. Despite many workers describing the common presence of
96 zoning in apatite and the use of BSE or CL techniques to observe the zoning (e.g.
97 Kempe and Goetze, 2002; Shore and Fowler, 1996), this first stage of apatite
98 description is often omitted and valuable information can therefore be missed.
99

100 **Trace elements**

101 A number of studies have presented detailed trace element chemistry for apatite
102 crystals in various igneous systems using in-situ techniques (e.g. Belousova et al.,
103 2001, 2002; Chu et al., 2009; Hoskin et al., 2000; Sha and Chappell, 1999). These
104 showed that rare earth element (REE) patterns vary with (i) the type of magma (e.g.
105 affected by differentiation, Hoskin et al., 2000), (ii) the presence or absence of other
106 accessory minerals (e.g. Hoskin et a., 2000; Miles et al., 2013) and could give clues
107 about (iii) the geological setting (Belousova et al., 2002; Chu et al., 2009; Sha and
108 Chappell 1999). More recently, detailed imaging associated with in-situ work has
109 shown that an important part of the crystallization history of an igneous body can
110 be observed at the apatite grain scale (e.g. Bruand et al., 2014, Zirner et al., 2015). In
111 the first part of this contribution, we summarize some of those findings and describe
112 their potential importance for a better understanding of petrogenetic processes.
113 Apatite chemistry from the high Ba-Sr granites (Northern Scotland, Bruand et al.,
114 2014) provide an excellent example to observes those new findings. Two localities

were studied in detail (the Strontian and Rogart plutons) in which compositions range from tonalitic to granodiorite to granite, with a local ultramafic component (the so-called appinites; Fowler et al., 2001, 2008). Results on the felsic compositions show that in one locality (Rogart) apatite displays oscillatory zoning and that REE content decreases continuously from core to rim, reflecting progressive in-situ crystal fractionation (Fig. 1b). By contrast, apatites from the second locality (Strontian) have oscillatory cores and homogeneous rims. These different zones correlate with an abrupt change in REE and Y, which is also visible in titanite from the same samples (decrease in REE, Nb and Ta). Prowatke and Klemme (2006) showed that apatite partition coefficients for REE are strongly dependent upon the SiO_2 content of the magma. Apatite in felsic systems can host up to almost an order of magnitude more REE than apatite crystallising in mafic systems (Fig. 2). Moreover, changes of REE, Zr, Nb and Ta in titanite and elemental ratios such as Sr/Sm in apatite and titanite match local apatite and titanite ultramafic compositions (See Fig. 6a, 7 and 12in Bruand et al., 2014). Therefore, these abrupt changes of apatite composition at Strontian are the likely result of a mixing event with local mafic magma, visible at the single grain scale in both apatite and titanite from the studied samples (Bruand et al., 2014), not apparent in whole –rock chemistry (Fowler et al., 2008) but in agreement with field evidence that shows disrupted synplutonic mafic dykes and abundant mafic enclaves.

Other trace elements in apatite have also proven useful to assess the host rock chemistry. A compilation of data from the literature indicates that the Sr content in

apatite is of particular interest (e.g. Jennings et al., 2011), since it correlates well with Sr of the whole rock (Fig. 3a). Importantly, Bruand et al. (2014) also showed that when Sr from the whole rock is affected by feldspar alteration (see altered sample on Fig. 3a), it is possible to estimate the original Sr content based on the SrAp content of the sample using the SrWR-SrAp correlation compiled from the literature . These authors also show that Sr content of apatite and titanite from the same samples correlate along a 10:1 regression line, which seems robust regardless of alteration in the whole rock. Sr in apatite has also been shown to correlate strongly with whole-rock SiO_2 (Fig. 3b; Belousova et al., 2001; Bruand et al., 2014, 2016; Jennings et al., 2011). Therefore, SiO_2 and Sr concentrations from the original rock can be derived using SrAp and give information of the original/unaltered host rock. This tool is important for future work on provenance studies (see second part of this paper).

Finally in this section, halogen (F, Cl) contents in apatite in igneous and metamorphic systems may ultimately be used as a proxy for water content of the melt. For example, the halogen content of apatites has been extensively used in the recent years to constrain the amount of water on the Moon (Boyce et al., 2010; Tartèse et al., 2013). However, there are still intense debates in the planetary science community as recent modelling work questions the reliability of water content estimates and infer that H-rich apatite can be generated from a magma poor in hydrogen (Boyce et al., 2014).

In situ isotopic analyses

O isotopes analyses in zircon have been used for many years to constrain the nature of the magma source reservoirs and more particularly the input of recycled material in the source or during assimilation (e.g. Valley et al., 2003 and references therein). Zircon has been shown to retain O isotope ratios of the magma source unlike other minerals in which O isotopes can be completely reset when affected by metamorphic or metasomatic events (e.g. quartz). Oxygen isotope data from single grains of other accessory minerals is limited (Bindeman, 2008). Although oxygen isotope analysis in bio-apatite is a common technique to interpret paleoenvironmental conditions (e.g. Zheng, 1996), data concerning metamorphic and magmatic rocks are almost non-existent (Farver and Giletti, 1989). Recent technical advances provide an opportunity to analyse in-situ O (King et al., 2001; Bonamici et al., 2014), Sm-Nd isotopes (Foster & Carter, 2007; Gregory et al., 2009), Cl and H isotopes in accessory minerals (e.g. Greenwood et al. 2011; Tartèse et al., 2014). Similarly, the understanding of oxygen isotope behaviour in other phases such as titanite has recently shown progress (e.g. King et al., 2001 for igneous and metamorphic rocks and Bonamici et al., 2011, 2014, 2015 for titanite in metamorphic rocks). King et al. (2001) show a consistent zircon-titanite fractionation factor of ~1.2 ± 0.3‰ for igneous and of ~2.1 ± 0.4‰ for metamorphic rocks. Bonamici et al. (2011, 2014) recently used oxygen isotope profiles in titanite grains to infer the cooling history of metamorphic rocks. In summary, although there is still a lot to learn about oxygen isotope behaviour in apatite, titanite or monazite, they have comparable potential to zircon (Valley, 2003) to highlight mantle and/or crustal components in the petrological source.

In terms of radiogenic isotopes, data are also limited, but Gregory et al. (2009) demonstrated that Sm-Nd isotope analysis at the micrometer scale offers the prospect of developing petrological tools similar to the current Hf isotope studies on zircons. They clearly show that Sm-Nd isotope analyses in titanite and apatite allow the estimation of the isotopic composition of the mantle or the crustal sources. Apatite, monazite and titanite have the advantage over zircon in being more widespread in less evolved magmas (e.g. Piccoli and Candela, 2002; Hoskin and Schaltegger, 2003) and being more responsive to igneous processes and crustal metamorphism (e.g. Bruand et al., 2014 for titanite and apatite; Rubatto et al., 2001 for monazite).

Potential for provenance studies?

Correlations detailed in Bruand et al. (2016; Sr-Ap vs SrWr, Sr-Ap vs SiO_2, Fig. 3) can be used to constrain the host rock composition of the studied minerals, even when they are detrital. Making use of such a tool could therefore be extremely valuable for future provenance studies. The majority of apatite provenance studies have focused on detrital thermochronology of apatite using fission track or U-Th/He thermochronometers (Bernet and Spiegel, 2004) and very little on trace elements. With the recent advances on the understanding of trace elements behaviour in apatite (Hoskin et al., 2000; Belousova et al., 2002; Chu et al., 2002; Jennings et al., 2011; Bruand et al., 2016), there would be merit to test in more details the robustness of trace elements in apatite during erosion, transport and diagenesis. However, apatite has been shown to be affected rapidly by metasomatism and

alteration (e.g. Zirner et al., 2015) given little hope to use it on a global scale in old terranes. Indeed, acidic groundwater, weathering and limited mechanical durability can affect the stability of apatite during sediment transport (Morton and Hallsworth, 2007). This severely limits its use as a detrital provenance tool. A novel way to look at apatite in the sedimentary record is to analyse apatite inclusions armoured within robust accessory minerals (e.g. zircon, titanite; Bruand et al., 2016; Darling et al., 2009; Jennings et al., 2011). The success of the method depends on the ability of apatite inclusions to record similar chemical features to those described above.

Apatite inclusions

Previously, inclusions present within datable accessory minerals such as zircon were viewed as a common problem, since they might introduce mixed ages and common Pb, which could lead to inaccurate and/or imprecise ages. The grains bearing those inclusions (Fig. 4) were therefore discarded. However, recent work has shown that these inclusions provide valuable insights into the history of a rock (e.g. Bruand et al., 2016; Darling et al., 2009; Jennings et al., 2011). While some inclusions (such as feldspar) have been shown to not reflect the original rock composition (Jennings et al., 2011), elements such as Sr has been shown to correlate with SrWR and SiO_2WR. In the first part of this contribution, we have shown that apatite composition gives additional petrogenetic information. In this part, we demonstrate how this petrogenetic history is also available *in apatite inclusions*

229 *armoured in zircon and titanite*, from which we can also recover an estimate of
230 whole rock composition.
231
232 **Apatite inclusions in zircons**
233 Apatite, micas, quartz and feldspar are common inclusions in igneous zircon (Fig.
234 5A). However, it has to be noted that careful counting of minerals in a set of samples
235 (Fig. 5A) indicates that the proportions of minerals as inclusions in zircons do not
236 necessary match their modal abundance (Darling et al., 2009). For example, quartz
237 is generally present in greater proportions compared with other phases as an
238 inclusion phase than within the matrix of the same rocks.
239
240 **From apatite inclusions to petrogenesis**
241 Apatite inclusions within titanites from a set of high Ba-Sr granitoids in Scotland
242 (Bruand et al., 2016; Fowler et al., 2001, 2008) have been imaged (Fig. 4) and
243 analysed using ion microprobe and electron microprobe techniques. Trace element
244 results confirm that the Sr concentrations of apatite inclusions and the Ce/Y ratios
245 correlate along a 1:1 correlation with those of apatite in the matrix (Bruand et al.,
246 2016; Fig. 6). Bruand et al. (2016) further demonstrate that the chemistry of apatite
247 provides important petrogenetic constraints for the plutons studied (e.g. insitu
248 crystal fractionation, mixing) that were not visible using whole rock data (Fowler et
249 al., 2001, 2008). In most cases, Sr in apatite has a homogeneous distribution (no
250 zoning), its concentration in apatite has been shown to be a function of plagioclase
251 fractionation during magmatic differentiation (Belousova et al., 2002). In contrast,

252 REE are extremely sensitive to changes in magmatic conditions. Prowatke and
253 Klemme (2005, 2006) demonstrated that apatite and titanite partition coefficients
254 for REE are dependent upon SiO_2 content. The REE partition coefficients for most
255 felsic rocks are higher than for mafic rocks, particularly for MREE. Therefore, ratios
256 such as Sr/Sm can be particularly helpful to discriminate different magma types. In
257 Figure 7, Sr/Sm of apatite inclusions and their titanite host minerals are reported.
258 They show that Sr/Sm in both minerals can discriminate mafic from felsic
259 (granitoid) compositions. The chemistries of titanite and apatite from the matrix
260 are also reported and show similar values. The studied samples show two different
261 crystallization histories. In Rogart, apatite and associated titanite zones have similar
262 Sr/Sm ratios and plot within a narrow range (Sr/Sm_{Ttn} ~ 0.05-0.12 and Sr/Sm_{Ap} ~
263 3-10). These results, associated with a continuous decrease of REE from core to rim,
264 suggest in-situ crystal fractionation. In Strontian, titanite cores and apatite
265 inclusions located in these cores plot in the same narrow field. On the other hand,
266 apatite inclusions in titanite rims and the associated titanite rims have systematic
267 higher Sr/Sm ratios (Fig. 7; Sr/Sm_{Ttn} >0.15 and Sr/Sm_{Ap} ~ 3-27). As discussed
268 above, this is interpreted to reflect a late influx of mafic magma during the
269 crystallization of Strontian granitoid (Bruand et al., 2014, 2016). Apatite and titanite
270 from the Strontian mafic-ultramafic facies (appinite) plot in the same region as the
271 titanite and apatite rims. In Strontian apatite and titanite record a general decrease
272 of REE from the inner toward the outer core of the titanite and then a late mixing
273 event with the local mafic magma within their rims. In summary, a detailed

snapshot of the petrogenetic history of a pluton is preserved within apatite inclusions in titanite or zircon.

From apatite inclusions to whole rock chemistry

Apatite chemistry is also extremely powerful for recovering information about the whole rock of their original host. For example, a global compilation of granitoids whole rock and apatite chemistry demonstrate a strong correlation between Sr_{Ap} and Sr_{WR} (Fig. 8), from which it is possible to "back calculate" Sr_{WR} based on apatite chemistry (Fig. 9). In Figure 8B, a compilation of post Archean samples and three average Archean tonalite trondjhemite granodiorite (TTG, black stars) compositions have been plotted, showing that Sr_{Ap} correlates with SiO_2 (Fig. 8B). As noted above, the studied high Ba-Sr granites (Bruand et al., 2016) systematically plot above the correlation defined by the other samples. This is consistent with whole-rock data. On Fig. 8C, the high Ba-Sr granites and their Archean equivalent (sanukitoids – Fowler and Rollinson, 2012) define an independent correlation. Based on these observations, a two-step method has been developed to recover original Sr and SiO_2 whole rock composition from Sr concentration in apatite.

- First, Sr_{WR} is back calculated using Sr_{Ap} and the correlation defined in Fig. 8A.
- Second, using this calculated Sr_{WR} value, the SiO_2 can be estimated (Fig. 8B). If $Sr_{WR} > 650$ ppm the correlation based on sanukitoid compilation is used and if $Sr_{WR} < 650$ ppm, the correlation based on the post-Archean trend is used. The 650 ppm cut off is based on the Sr_{WR} value of the most mafic endmember of the post-Archean trend.

297

298 Following this procedure, appropriate partition coefficients can be chosen (e.g. Luhr
299 et al., 1984; Prowatke and Klemme, 2005, 2006) and the REE of the host magma can
300 be calculated, which is broadly equivalent to that of the whole host rock. For
301 example, results for Rogart are shown in Fig. 9 (whole-rock data from Fowler et al.,
302 2008). Apatite and titanite produce similar results and a particularly good fit for
303 sample RHG1. The results from Strontian produce a good fit for sample SR4 for
304 apatite inclusions from the core and the titanite core composition (higher REE
305 contents of the calculated area in Fig. 9). Calculated MREE concentrations for SR1
306 and SR3 are generally lower than that of the whole rock. This could be explained by
307 a slight discrepancy between the partition coefficient for apatite and titanite that we
308 used and our sample. Calculations made with rim compositions plot at much lower
309 REE and their calculated REE patterns give lower values especially for MREE (Fig.
310 9). When this back-calculation method is used on grains that have been affected by
311 the complications of a late influx of mafic magma such as in Strontian (Figs. 1, 7),
312 only the unaffected core composition should be used for calculations. Although
313 clearly not perfect, key elemental ratios such as Ce/Yb and Eu/Eu* are accurately
314 reproduced. Thus, it seems likely that apatite and titanite have the potential to
315 faithfully record their parent melt chemical signature.

316

317 **Apatite inclusions in zircon and titanite – a window to the early Earth?**

318 Robust detrital accessory minerals such as monazite and zircon preserved in
319 sandstones are particularly informative as they can be dated and can then be

potentially compared to similar terranes to allow paleogeographic reconstruction (e.g. Samson et al., 2005). Much of what we know about early crustal evolution and the generation of continents is based on such work. However, zircon trace element chemistries have not yet been proven particularly helpful to discriminate different magma compositions and allow a detailed interpretation of their original host rock (e.g. Coogan and Hinton, 2006), which represents a major weakness in the approach. We have shown above that it is possible to reconstruct whole rock chemistry of the parent rock (Belousova et al., 2002; Bruand et al., 2016; Jennings et al., 2011) based on apatite chemistry, even when the crystals are <100 microns inclusions in other accessory minerals. Such work could be applied to inclusions in the detrital zircon archive, such that magmatic composition over time could be recovered. Of particular interest in this regard, is the presence of apatite inclusions reported in the oldest terrestrial zircons from Jack hills (Hopkins et al., 2008; Rasmussen et al., 2011). Rasmussen et al. (2011) report the presence of numerous inclusions that are secondary and have crystallized during one of the later metamorphic events, some of them replacing apatite (e.g. xenotime, monazite, muscovite; Fig. 5B). However, they also report the presence of rare preserved primary apatite, whose petrogenetic affinities would be illuminating.

Implications

Apatite chemistry has the ability to record petrogenetic processes that are not available using whole rock data. It also discriminates different magma composition

that are diagnostic of geodynamic changes during crustal evolution (e.g. distinguish sanukitoids from post-Archean granitoids). Between the Archean (4-2.5 Ga ago) and the Phanerozoic (0.54 Ga to present), the magmatic production system changed from a "hot" Earth, producing TTG suites, to a 'colder' Earth, producing mainly calc-alkaline andesitic crust (e.g. Martin et al., 2005). This shift of composition has been interpreted by some as reflecting major geodynamic changes of the Earth and ultimately has been linked to the onset of plate tectonic (Martin et al., 2005). Sanukitoids are interpreted as being the product of a metasomatized mantle wedge and have been reported as occurring during the Archean-Proterozoic transition (~2.7-2.5 Ga; Martin *et al.*, 2009). They have been interpreted by various workers (e.g. Martin *et al.*, 2009) as the result of the evolution from a shallow to a steep subduction style in this time interval and therefore might mark the onset of modern plate tectonics. However, there are remaining fundamental unknowns about the conditions of the early Earth as its record is extremely sparse (Bleeker et al., 2005; e.g. composition of the crust, geodynamic regime). The study of accessory minerals and more particularly detailed in-situ work on apatite (trace element and isotopes) provides a potentially pivotal role to gather more information about igneous processes and to interrogate the rock record in ever greater detail (e.g. Hadean zircons, eroded products of ancient cratons). Although there has been a recent increase in work on REE in apatite and other accessory minerals, there is still much to do. For example:

- Studying in greater detail REE behaviour in the whole set of accessory minerals in various magma compositions. Most studies focus on one of the accessory phases

contained within a suite of rocks (e.g. Tepper & Kuehner, 1999; McLeod *et al.*, 2011). The comparison of the different accessory phases within a suite of samples is more rarely done (Bruand et al., 20015; Hoskin *et al.*, 2000b). As those minerals all bear REE, systematic comparative studies are essential to understand their behaviour.

- Improving the understanding of redox sensitive elements in apatite (S, Mn; Miles et al., 2014; Parat et al., 2011)
- Studying less investigated elements such as Pb, Sr, Th, Nb, U, V and Ta that are also sensitive to changes in magma composition.

Acknowledgments

We are grateful to Stuart Kearns for the help provided with the microprobe analyses, Tony Butcher for assistance during the SEM and cathodoluminescence work and Geoff Long for technical support. We are extremely grateful to the EIMF (Edinburgh Ion Microprobe Facility) for the help provided with the ion probe analyses. We wish to thank the Selfrag Company (Kerzers, Switzerland) for help during the preparation of the samples. This work was supported by the Natural Environment Research Council [Grant number NE/I025573/1], and is a contribution to International Geoscience Programme (IGCP) 599.

References cited

388 Belousova, E. A., Walters, S., Griffin, W. L. and O'Reilly, S. Y. (2001) Trace-element
389 signatures of apatites in granitoids from the Mt Isa Inlier, northwestern Queensland.
390 Australian. Journal of Earth Sciences, 48, 603-619.
391 Belousova, E.A., Griffin, W.L., O'Reilly, S.Y. and Fisher, N.I. (2002) Apatite as an
392 indicator mineral for mineral exploration: trace-element compositions and their
393 relationship to host rock type. Journal of Geochemical Exploration, 76, 45-69.
394 Bindeman, I. (2008) Oxygen isotopes in mantle and crustal magmas as revealed by single
395 crystal analysis. Reviews in Mineralogy and Geochemistry, 69, 445-478.
396 Bonamici, C., Kozdon, R., Ushikubo, T. and Valley, J.W. (2011) High-resolution P-T-t
397 paths from $\delta^{18}O$ zoning in titanite: A snapshot of late-orogenic collapse in the
398 Grenville of New York. Geology, 39, 959-962.
399 Bonamici, C., Kozdon, R., Ushikubo, T. and Valley, J.W. (2014) Intragrain oxygen
400 isotope zoning in titanite by SIMS: Cooling rates and fluid infiltration along the
401 Carthage-Colton Mylonite Zone, Adirondack Mountains, NY, USA. Journal of
402 metamorphic Geology, 32, 71-92.
403 Bonamici, C., Fanning, C.M., Kozdon, R., Fournelle, J.H. and Valley, J.W. (2015)
404 Combined oxygen-isotope and U-Pb zoning studies of titanite: new criteria for
405 age preservation. Chemical Geology, 398, 70-84.
406 Boyce, J.W., Liu, Y., Rossman, G.R., Guan, Y., Eiler, J.M., Stolper, E.M. and Taylor,
407 L.A., (2010) Lunar apatite with terrestrial volatil abundances. Nature, 466, 466-
408 69.
409 Boyce, J.W., Tomlinson, S.M., McCubbin, F.M., Greenwood, J.P. and Treiman, A.H.
410 (2014). The Lunar apatite paradox. Science, 344, 400-402.

411 Bruand, E., Storey, C. and Fowler, M. (2014) Accessory mineral chemistry of High Ba-Sr
412 granites from northern Scotland: constraints on petrogenesis and records of
413 whole-rock signature. Journal of Petrology, 55, 1619-1651.
414 Bruand, E., Storey, C. and Fowler, M. (2016) Apatite inclusions within zircon and titanite
415 as a window into the early Earth. Geology, 44, 91-94.
416 Chew, D. and Donelick, R. (2012) Combined apatite fission track and U-Pb dating by
417 LA-ICP-MS and its application in apatite provenance analysis. Mineralogical
418 Association of Canada Short Course, 42, 219-247.
419 Chu, M.F., Wang, K.L., Griffin, W.L., Chung, S.L., O'Reilly, S.Y., Pearson, N.J. and
420 Iizuka, Y. (2009) Apatite Composition: Tracing Petrogenetic Processes in
421 Transhimalayan Granitoids. Journal of Petrology, 50, 1829-1855.
422 Coogan, L.A. and Hinton, R. (2006) Do the trace element compositions of detrital zircons
423 require Hadeaan continental crust? Geology, 34, 633-636.
424 Darling, J., Storey, C. and Hawkesworth, C. (2009) Impact melt sheet zircons and their
425 implications for the Hadean crust. Geology, 37, 927–930, DOI:10.1130/G30251A.1.
426 Farver, J.R. and Giletti, B.J. (1989) Oxygen and strontium diffusion kinetics in apatite
427 and potential applications to thermal history determinations. Geochimica and
428 Cosmochimica Acta, 53, 1621-1631.
429 Foster, G. and Carter, D. (2007) Insights into the patterns and locations of erosion in the
430 Himalaya - A combined fission-track and in situ Sm-Nd isotopic study of detrital
431 apatite. Earth Planetary Science Letters, 257, 407-418.

Fowler, M. B., Henney, P. J., Darbyshire, D. P. F. and Greenwood, P. B. (2001) Petrogenesis of high Ba-Sr granites: the Rogart pluton, Sutherland. Journal of the Geological Society, 158, 521-534.

Fowler, M. B., Kocks, H., Darbyshire, D. P. F. and Greenwood, P. B. (2008) Petrogenesis of high Ba-Sr plutons from the Northern Highlands Terrane of the British Caledonian Province. Lithos, 105, 129-148.

Fowler, M. and Rollinson, H. (2012) Phanerozoic sanukitoids from Caledonian Scotland: Implications for Archean subduction. Geology, 40, 1079-1082.

Greenwood, J. P., Itoh, S., Sakamoto, N., Warren,, P., Taylor L. A. and Yurimoto H. (2011) Hydrogen isotope ratios in lunar rocks indicate delivery of cometary water to the Moon. Nature Geoscience, 4, 79–82.

Gregory, C.J., McFarlane, C.R.M., Hermann, J. and Rubatto, D. (2009) Tracing the evolution of calc-alkaline magmas: In-situ Sm-Nd isotope studies of accesory minerals in the Bergell Igneous Complex, Italy. Chemical Geology, 260, 73-86.

Harlov, D. E. (2015) Apatite; a fingerprint for metasomatic processes (in Apatite; a mineral for all seasons). Elements Magazine, 11(3),171-176

Hopkins, M.D., Harrison, T.M. and Manning, C.E. (2010) Constraints on Hadean geodynamics from mineral inclusions in>4 Ga zircons. Earth and Planetary Science Letters, 298, 367-376.

Hoskin, P.W.O. and Ireland, T.R. (2000a) Rare earth element chemistry of zircon and its use as a provenance indicator. Geology, 28, 627-630.

453 Hoskin, P.W.O., Kinny, P.D., Wyborn, D. and Chappell, B.W. (2000b) Identifying
454 accessory mineral saturation during differentiation in granitoid magmas: an
455 integrated approach. Journal of Petrology, 41, 1365-1396.
456 Iizuka, T., Nebel, O. and McCulloch, M.T. (2011) Tracing the provenance and
457 recrystallization processes of the Earth's oldest detritus at Mt. Narryer and Jack
458 Hills, Western Australia: An in situ Sm-Nd isotopic study of monazite. Earth and
459 Planetary Science Letters, 308, 350-358.
460 Jennings, E.S., Marschall, H.R., Hawkesworth, C.J. and Storey, C.D. (2011)
461 Characterization of magma from inclusions in zircon: Apatite and biotite work
462 well, feldspar less so. Geology, 39, 863-866.
463 King, E.M., Valley, J.W., Davis, D.W. and Kowallis, B.J. (2001) Empirical
464 determination of oxygen isotope fractionation factors for titanite with respect to
465 zircon and quartz. Geochimica et Cosmochimica Acta, 65, 3165-75.
466 Kempe, U. and Götze, J. (2002) Cathodoluminescence (CL) behaviour and crystal
467 chemistry of apatite from rare-metal deposits. Mineralogical Magazine, 66, 135–
468 156.
469 Luhr, J. F., Carmichael, I. S. E. and Varekamp, J. C. (1984) The 1982 eruptions of el-
470 chichon volcano, chiapas, mexico - mineralogy and petrology of the anhydrite-
471 bearing pumices. Journal of Volcanology and Geothermal Research, 23, 69-108.
472 Martin, H., Moyen, J.F. and Rapp, R. (2009) The sanukitoid series: Magmatism at the
473 Archean-Proterozoic transition. Earth and Environmental Science Transactions of
474 the Royal Society of Edinburgh, 100, 15–33, DOI:10.1017/S1755691009016120.

McCubbin, F.M. and Jones, R.H. (2015) Extraterrestrial apatite: Planetary geochemistry to astrobiology. Elements Magazine, 11, 183–188, DOI:10.2113/gselements.11.3.183.

McDonough, W.F., and Sun, S.S. (1995) The Composition of the Earth. Chemical Geology, 120, 223–253, DOI:10.1016/0009-2541(94)00140-4.

Miles, A. J., Graham, C. M., Hawkesworth, C. J., Gillespie, M. R. and Hinton, R. W. (2013) Evidence for distinct stages of magma history recorded by the compositions of accessory apatite and zircon. Contributions to Mineralogy and Petrology, 166, 1-19.

Miles, A.J., Graham, C.M., Hawkesworth, C.J., Gillespie, M.R. and Hinton, R.W. (2014) Mn in apatite: A new redox proxy for silicic magmas? Geochimica et Cosmochimica Acta, 132, 101-119.

Morton, A. and Hallsworth, C. (2007) Stability of detrital heavy minerals during burial diagenesis, in Mange, M., and Wright, D.K., eds., Heavy Minerals in Use: Amsterdam, Elsevier, Developments in Sedimentology, 58, 215–245, DOI:10.1016/S0070-4571(07)58007-6.

Parat F., Holtz F. and Streck M. (2011) Sulfur-bearing magmatic accessory minerals. In : Behrens H, Webster JD (eds) Sulfur in Magmas and Melts and Its Importance for Natural and Technical Processes. Reviews in Mineralogy and Geochemistry, 73, 285-314.

Piccoli, P., Candela, P. and Rivers, M. (2000) Interpreting magmatic processes from accessory phases: titanite- a small scale recorder of large-scale processes. Geological Society of America Special Papers, 350, 257-267.

498 Prowatke, S. and Klemme, S. (2005) Effect of melt composition on the partitioning of
499 trace elements between titanite and silicate melt. Geochimica Et Cosmochimica
500 Acta, 69, 695-709.
501 —, (2006) Trace element partitioning between apatite and silicate melts. Geochimica Et
502 Cosmochimica Acta, 70, 4513-4527.
503 Rasmussen, B., Fletcher, I.R., Muhling, J.R., Gregory, C.J. and Wilde, S. (2011)
504 Metamorphic replacement of mineral inclusions in detrital zircon from Jack Hills,
505 Australia: Implications for the Hadean Earth. Geology, 39, 1143-1146.
506 Rubatto, D., Williams, I.S. and Buick, I.S. (2001) Zircon and monazite response to
507 prograde metamorphism in the Reynolds Range, central Australia. Contributions
508 to Mineralogy and Petrology, 140, 458-468.
509 Sha, L. K. and Chappell, B. W. (1999) Apatite chemical composition, determined by
510 electron microprobe and laser-ablation inductively coupled plasma mass
511 spectrometry, as a probe into granite petrogenesis. Geochimica Et Cosmochimica
512 Acta 63, 3861-3881.
513 Shore, M. and Fowler, A.D. (1996) Oscillatory zoning in minerals; A common
514 phenomenon. Canadian Mineralogist, 34, 1111–1126.
515 Tartèse, R., Anand, M., McCubbin, F.M., Elardo, S.M., Shearer, C.K. and Franchi, I.A.
516 (2014) Apatites in lunar KREEP basalts: The missing link to understanding the H
517 isotope systematics of the Moon. Geology, 42, 363-66.
518 Tepper, J. H. and Kuehner, S. M. (1999) Complex zoning in apatite from the Idaho
519 batholith: A record of magma mixing and intracrystalline trace element diffusion.
520 American Mineralogist, 84, 581-595.

Valley, J.W. (2003) Oxygen isotopes in zircon. Reviews in Mineralogy and Geochemistry, 53, 343-385.

Webster, J.D. and Piccoli, P.M. (2015) Magmatic apatite: a powerful yet deceptive, Mineral. Elements Magazine, 11, 177-182.

Wilde, S.A., Valley, J.W., Peck, W.H. and Graham, C.M. (2001) Evidence from detrital zircons for the existence of continental crust and oceans on the Earth 4.4 Gyrs ago. Nature, 409, 175-178.

Zheng, Y-F. (1996) Oxygen isotope fractionations involving apatites: Application to paleotemperature determination. Chemical Geology,127, 177-187.

Zirner, A., Marks, M., Wenzel, T., Jacob, D. and Markl, G. (2015) Rare earth elements in apatite as a monitor of magmatic and metasomatic processes: The llimauussaq complex, South Greeland. Lithos, 228-229, 12-22.

Figure Captions

Figure 1. Modified after Bruand et al. (2014). Cathodoluminescence images of apatites crystals for granitoids (A-B). A- Apatites from Strontian granitoids are made up of oscillatory cores and unoscillatory rims. These two zones correspond to a sudden change of apatite chemistry and more particularly a decrease of REE. The rim records a mixing event with local mafic magma. B- Apatites from Rogart granitoids are characterized by an oscillatory zoning. Apatite REE concentration continuously decreases from core to rim reflecting progressive in situ crystal fractionation.

544 Figure 2. Apatite/ melt partition coefficient for apatite for felsic and mafic
545 compositions (modified after Prowatke & Klemme, 2006).
546
547 Figure 3. SrAp-SrWR and SrAp-SiO_2 compilation. Data from Hoskin et al., 2000b
548 (black dot), Chu et al., 2009 (grey dot), Jennings et al., 2011 (colourless dot),
549 Belousova et al., 2001 (cross) and Bruand et al., 2014 (square). A- SrAp-SrWR
550 showing close correlation. B- SrAp-SiO_2WR showing broad correlation. Obvious
551 outliers are the high Ba-Sr granites from Bruand et al. (2014).
552 Figure 4. Apatite inclusions and host minerals (zircon and titanite). Analysis
553 numbers available in tables DR1-DR2 in Bruand et al., (2016).
554
555 Figure 5. Zircon inclusion populations. A- After Darling et al. (2009). Left: relative
556 frequency of main inclusion phases in various rock types. Right: Streckeisen
557 diagram showing rock and inclusion mineralogy for each sample. Arrows indicate
558 different proportion of minerals from whole rock to zircon inclusions. B-After
559 Rasmussen et al. (2011) in repository material. Mineral and mineral inclusions data
560 for the Jack Hills (JH) and the Narryer Gneiss Complex (NGC).
561
562 Figure 6. Inclusions in zircon-titanite versus rock matrix. Data are average
563 compositions given with 2 sigma errors. A) Ce/Y apatite. B) Sr apatite. After Bruand
564 et al. (2016)
565

566 Figure 7. Petrogenetic processes and the nature of the parent magma (granitoid
567 versus mafic) using Sr/Sm ratios in apatite inclusions and host titanite. For
568 comparison, apatite and titanite average compositions from the matrix have also
569 been reported (error bars are 1σ, Bruand et al., 2014, 2016).
570
571 Figure 8. A- $Sr_{Apincl.}$ average compositions versus Sr_{WR} (error bars are 2σ). Available
572 data on post Archean granitoids (crosses – Jennings et al., 2011; Belousova et al,
573 2002; Chu et al., 2009; Hoskin et al., 2000; square- Rogart locality and diamond-
574 Strontian locality in high Ba-Sr granites from Bruand et al., 2016) have been added.
575 B- Sr_{Ap} vs SiO_{2WR} with apatite inclusions in the grey field of the studied high Ba-Sr
576 samples (sanukitoid-like, 2σ error bars) and two sanukitoids from the Karelian
577 Province analyzed by electron microprobe, and Post-Archean apatite data set in the
578 white field. C- Sr_{WR} vs SiO_{2WR} with the sanukitoid compilation (Fowler and Rollinson,
579 2012 ; SiO_{2WR}>46%), the high Ba-Sr granites (Fowler et al., 2001, 2008), average
580 TTG compositions from Martin et al. (2005) and the Post-Archean data set. This
581 Figure is after Bruand et al. (2016).
582
583 Figure 9. Back-calculation of parent magma composition using single apatite
584 inclusions and titanite in host rock analysis (Bruand et al., 2016 dataset). KD values
585 of Luhr et al., (1984) for apatite and titanite. For comparison, sanukitoid data set
586 from Martin et al. (2009) has been added. Chondrite values are from Mc Donough
587 and Sun (1995).
588

589

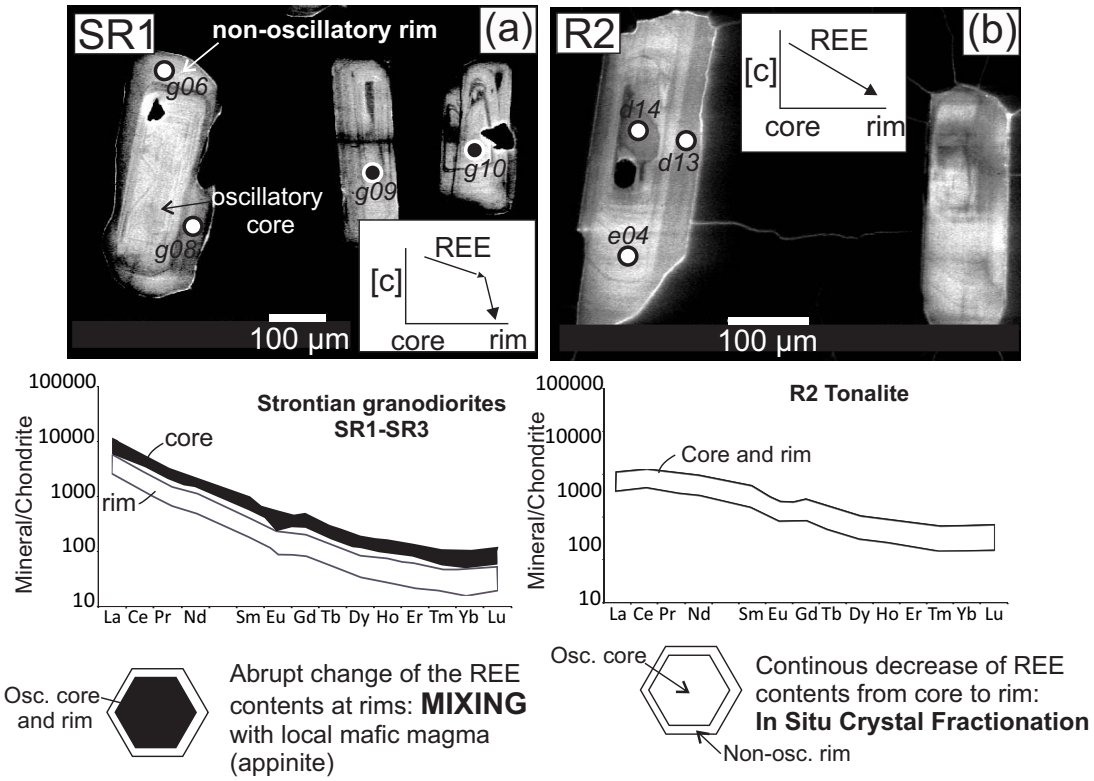

Fig. 1

Fig. 1, Bruand et al. (2016)

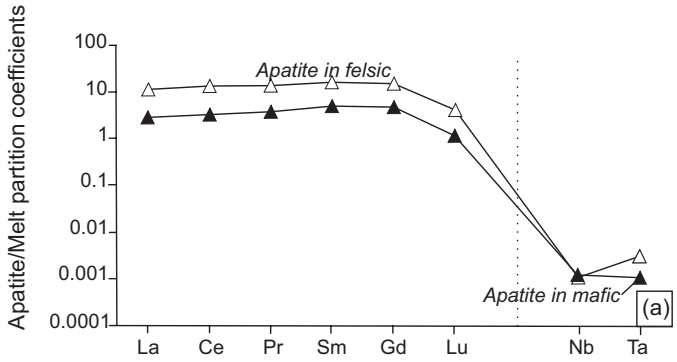

Fig. 2 Bruand et al. (2016)

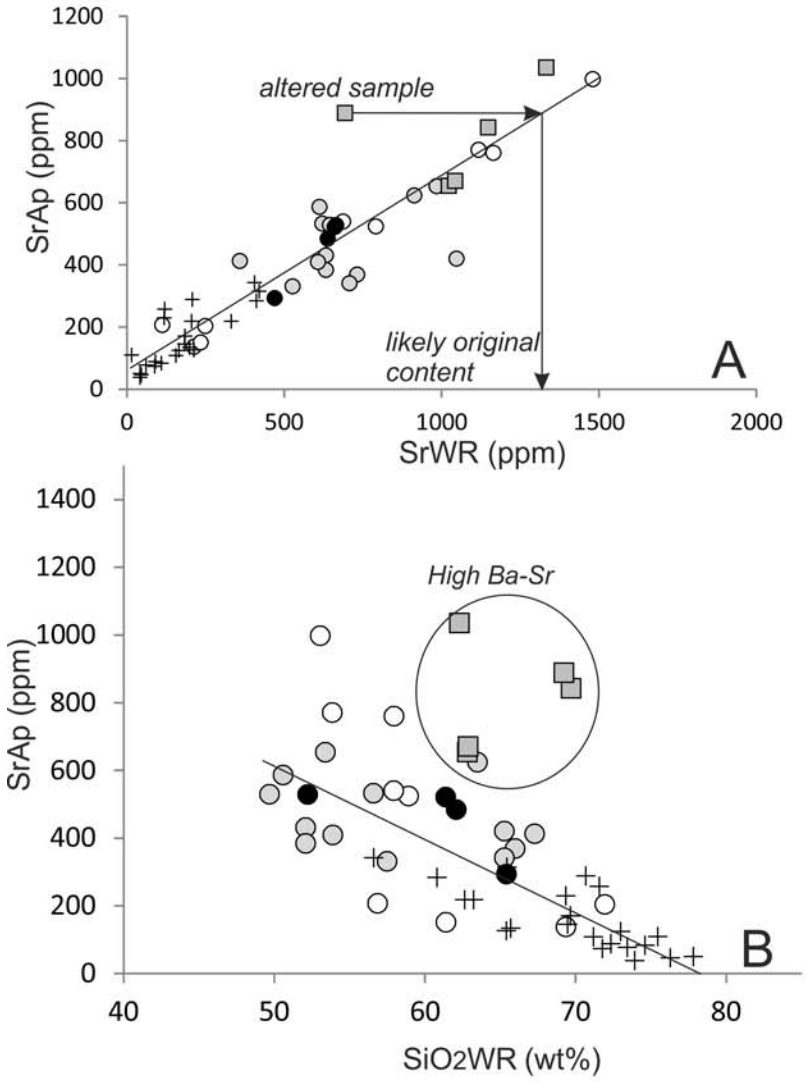

Fig. 3, Bruand et al (2016)

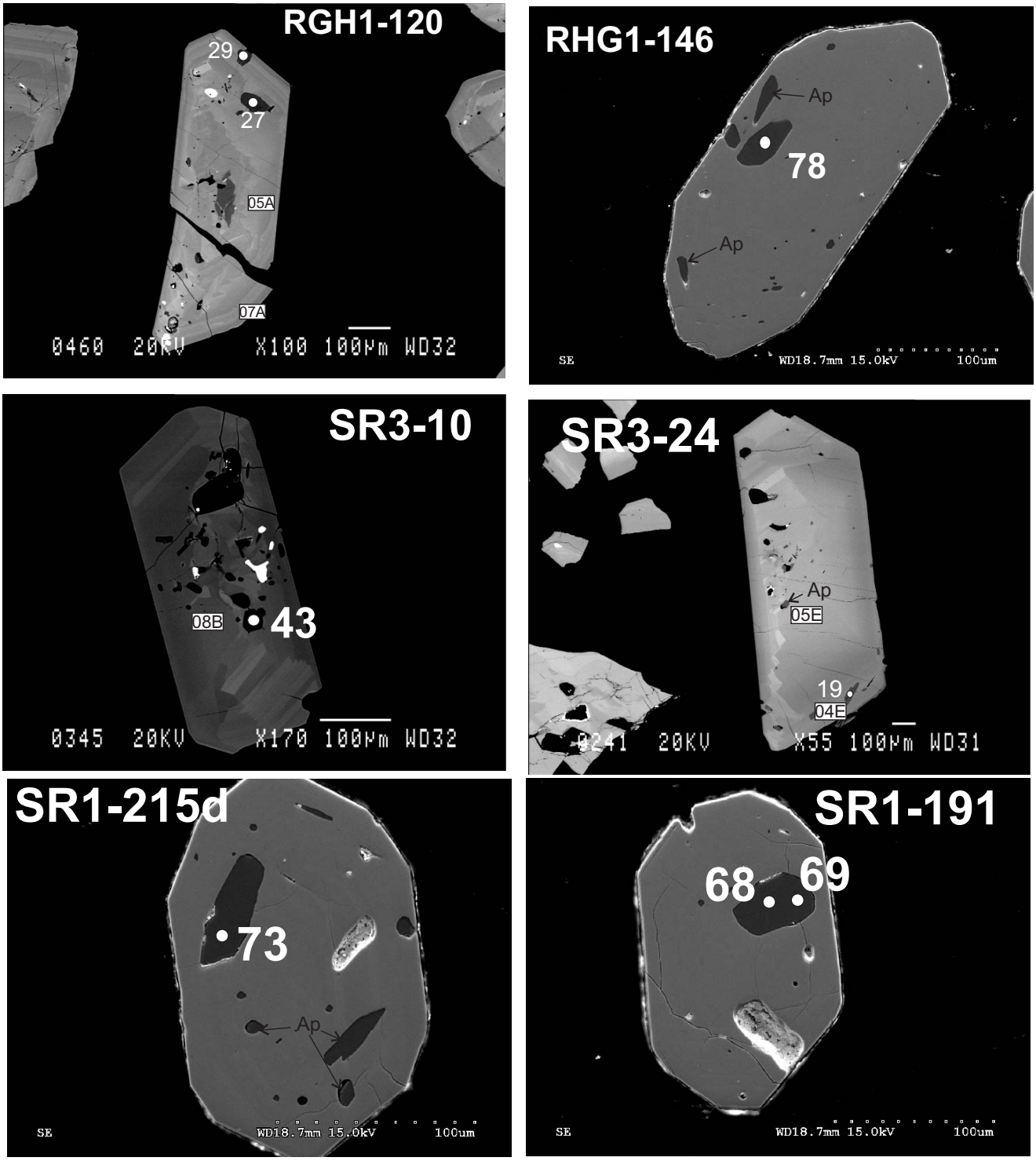

Fig. 4, Bruand et al. (2016)

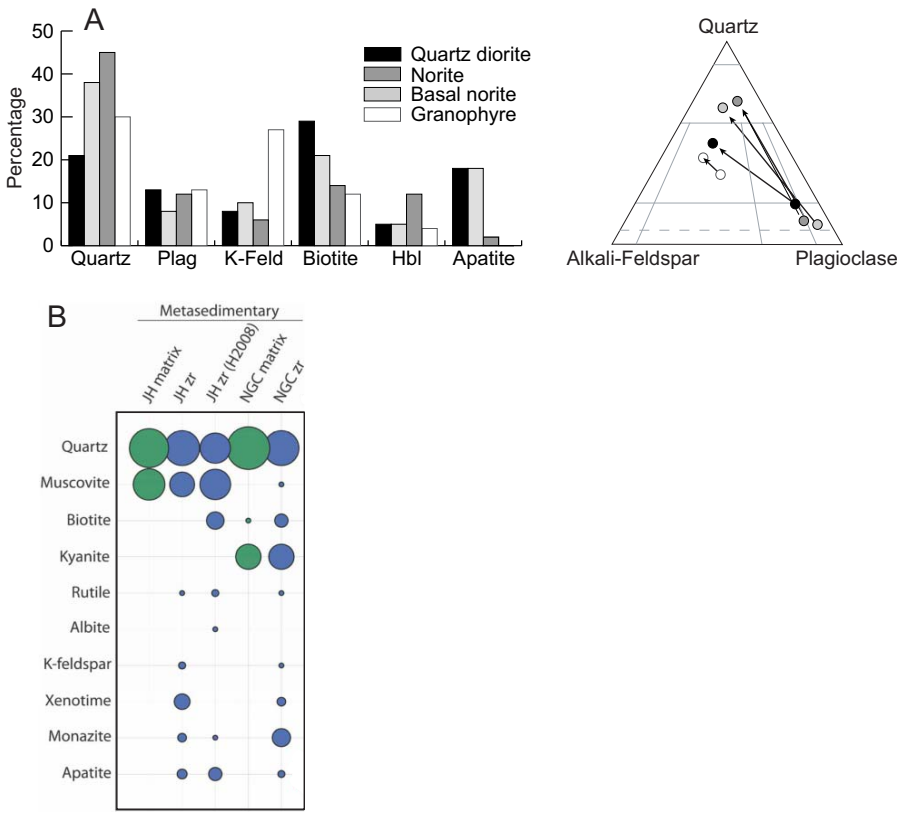

Fig. 5, Bruand et al (2016)

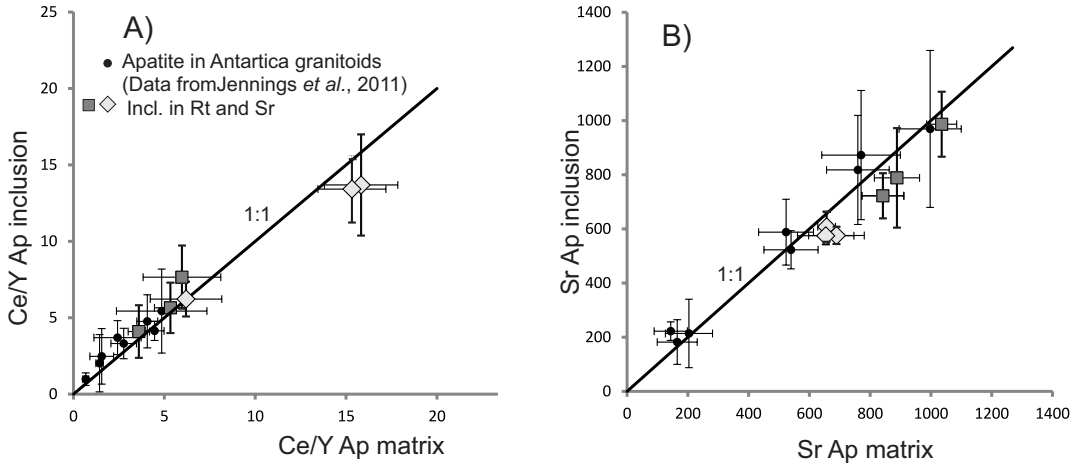

Fig. 6, Bruand et al. (2016)

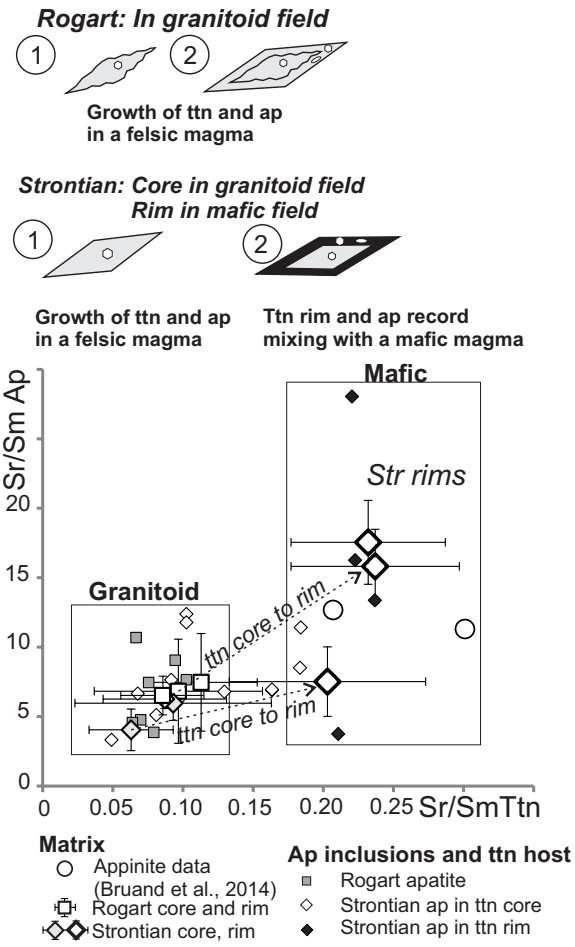

Fig.7 Bruand et al., 2016

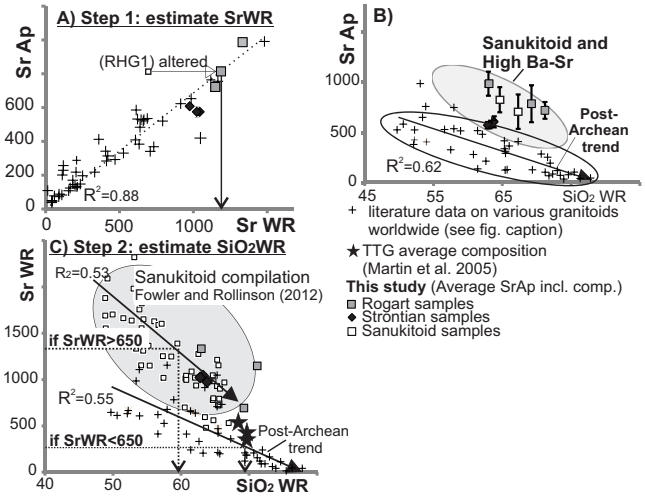

Fig. 8 Bruand et al. (2016)

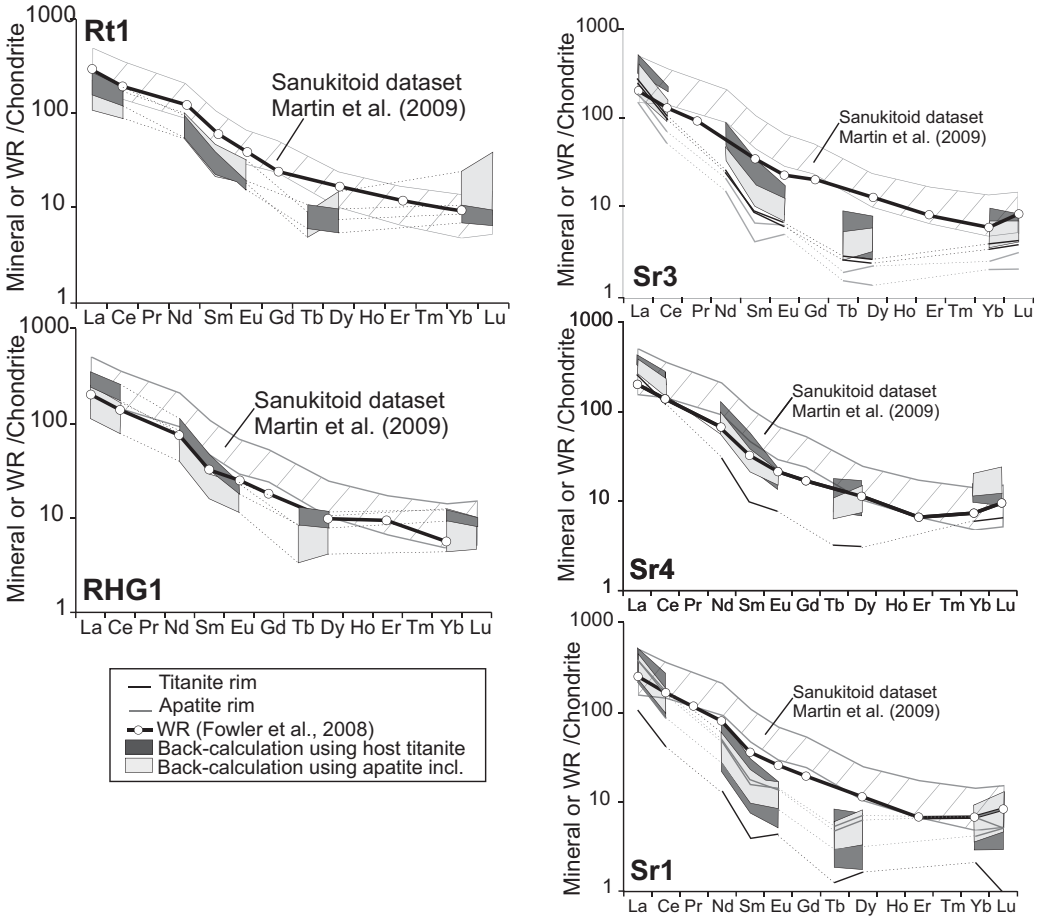

Fig. 9, Bruand et al (2016)